



ELSEVIER

Contents lists available at ScienceDirect

Physica B

journal homepage: [www.elsevier.com/locate/physb](http://www.elsevier.com/locate/physb)

# Structural, electronic and magnetic properties of negative thermal expansion material $\text{Mn}_3\text{Cu}_{1-x}\text{Sn}_x\text{N}$

L. Hua\*, J. He

Department of Applied Physics, Taizhou college of Nanjing Normal University, Taizhou 225300, China

## ARTICLE INFO

### Article history:

Received 28 November 2010

Received in revised form

27 December 2010

Accepted 28 December 2010

Available online 5 January 2011

### Keywords:

Antiperovskite structure

Density of states

Fermi level

Electronic and magnetic properties

## ABSTRACT

We have investigated the structural, electronic and magnetic properties of  $\text{Mn}_3\text{Cu}_{1-x}\text{Sn}_x\text{N}$  ( $x=0, 0.5$ ) using first-principles density functional theory within the generalized gradient approximation (GGA) + U schemes. The crystal structure of the compounds is tetragonal crystal for  $x=0$  while it is a cubic crystal for  $x=0.5$ . Our spin-polarized calculations give a metallic ground state for the  $x=0, 0.5$  in agreement with experiments. From the charge density and density of states (DOS), the coupling between Sn 5p with Mn 3d and spin geometrical frustration effect are the main reasons for magnetic transition in  $\text{Mn}_3\text{Cu}_{1-x}\text{Sn}_x\text{N}$ .

© 2010 Elsevier B.V. All rights reserved.

## 1. Introduction

Negative thermal expansion (NTE), the decrease in volume or length of a material with increasing temperature, is an unusual property exhibited by relatively few materials [1–4]. The phenomenon is known to arise from a range of different physical mechanisms, including magnetostriction in ferromagnetic materials [5], valence transitions in intermetallic [6] and fullerene materials [7]. NTE materials can compensate or control (positive) thermal expansion of materials by forming composites, which have been widely used as, for example, high-precision (zero-expansion) optical and machinery parts [8,9].

An important mechanism of NTE is the magnetovolume effect (MVE). With decreasing temperature ( $T$ ), the volume can be expanded gradually by changing the amplitude of the magnetic moment. This MVE of itinerant electron systems has been investigated since the discovery of extraordinarily small thermal expansion in Invar alloys [10]. However, in many materials which exhibit large MVEs, the volume expansion is very sharp against  $T$  because the ordered magnetic moment rapidly increases below the magnetic transition temperature. The volume expansion can be even discontinuous when the magnetic transition is first order. Then MVE must be broadened against  $T$  in order to obtain the material with the negative or zero-thermal expansion. One of recent technological essence is the discovery of Ge dopant that broadens the sharp volume contraction due to the first-order

magnetic transition from low- $T$  antiferromagnetic (AFM) to high- $T$  paramagnetic (PM) state of the stoichiometric antiperovskites  $\text{Mn}_3\text{AN}$  ( $A=\text{Zn}, \text{Ga}, \text{etc.}$ ) [11,12]. Recently, Takenaka et al. have systematically investigated effects of Sn doping on thermal expansion of  $\text{Mn}_3\text{CuN}$  and found that Tin also broadens the volume change at the magnetic transition [13]. However, we found that they have successfully obtained the broadening of MVE in antiperovskite  $\text{Mn}_3\text{CuN}$  by the substitution of only Ge and Sn atoms for Cu until now. This is one of the mysteries and, hence, the physical as well as chemical roles of this magic element Ge are now being studied from the various points of view [14,15]. Iikubo et al. believed that not only a cubic crystal structure but also a  $I^{5g}$  antiferromagnetic spin structure are key ingredients of the large magnetovolume effect in this itinerant electron system and a local lattice distortion of tetragonal ( $T_4$ ) structure of  $\text{Mn}_3\text{GeN}$  in  $\text{Mn}_3\text{Cu}_{1-x}\text{Ge}_x\text{N}$  is considered to trigger the broadening of the volume change [16,17]. To our knowledge, there is no calculations on the  $\text{Mn}_3\text{Cu}_{1-x}\text{Sn}_x\text{N}$  until now. In this paper, we perform density-functional electronic structure calculations on  $\text{Mn}_3\text{Cu}_{1-x}\text{Sn}_x\text{N}$  ( $x=0, 0.5$ ) and clarify the role of Tin-doping effect in the mechanism of structure and magnetic transition.

## 2. Computational details

Our calculations are performed using the projector augmented wave (PAW) method [18], as implemented in the VASP code [19]. The plane-wave cutoff energy is 400 eV. The exchange correlation potential is treated by the generalized gradient approximation with Perdew–Burke–Ernzerhof parameterization [20]. In order to

\* Corresponding author. Tel.: +86 0523 86153922.  
E-mail address: pjsd@163.com (L. Hua).

assess the magnetic state of Mn in  $\text{Mn}_3\text{Cu}_{1-x}\text{Sn}_x\text{N}$ , the spin-polarized calculations are also performed. To correct the on-site Coulomb interaction of the Mn 3d orbital, the GGA+U method is employed with  $U=2.0$  eV and  $J=0.9$  eV (i.e.  $U_{\text{eff}}=1.1$  eV) for the Mn 3d orbital. 3d4s for Mn, 3d4s for Cu, 5s5p for Sn, 2s2p for N are treated as valence orbitals in the calculations. Brillouin zone sampling is performed on a Monkhorst–Pack (MP) mesh [21] of  $4 \times 4 \times 4$ . Bulk and Sn doping calculations are performed in a  $2 \times 2 \times 1$  supercell with 20 atoms. Forces on atoms are calculated and atoms are allowed to relax using a conjugate gradient technique until their residual forces have converged to less than  $0.01$  eV/Å. For  $\text{Mn}_3\text{Cu}_{1-x}\text{Sn}_x\text{N}$  ( $x=0.5$ ), we substitute two Cu atoms with Sn to form  $\text{Mn}_3\text{Cu}_{0.5}\text{Sn}_{0.5}\text{N}$ .

### 3. Results and discussion

We have constructed a  $2 \times 2 \times 1$  supercell consisting of 20 atoms with three inequivalent Mn sites at Mn1(0, 0.5, 0.5), Mn2(0.5, 0, 0.5) and Mn3(0.5, 0.5, 0) positions for the bulk sample as shown in Fig. 1. For  $\text{Mn}_3\text{Cu}_{0.5}\text{Sn}_{0.5}\text{N}$ , there are two kinds of inequivalent Sn site substitutions which are along the [0 1 0] and [1 1 0] directions, respectively. We calculate the total energy of two kinds of inequivalent Sn site substitutions and find that the supercell with Sn site substitution along the [0 1 0] direction owns the lowest total energy. Thus we select this kind of Sn site substitution as our *ab initio* calculations.  $\text{Mn}_3\text{CuN}$  have a tetragonal structure (space group: P4/mmm) and the magnetic unit cell of the low temperatures FM phase is two times enlarged within the *ab* plane, containing six manganese atoms or magnetic moments. Four moments are canceled out within the *ab* plane, while two moments are ferromagnetically aligned along the *c* axis [16]. Sn doping samples have a cubic structure (space group: Pm $\bar{3}$ m). The total magnetic moment approximates zero while magnetic structure is yet to be confirmed [13]. But the present study shows that the  $\Gamma^{5g}$  triangular AFM spin configuration as well as the cubic crystal structure are key ingredients for the pronounced MVE, typically for  $\text{Mn}_3\text{Cu}_{1-x}\text{Ge}_x\text{N}$  [16]. The Table 1 lists calculated structural parameters and total magnetic moments for  $\text{Mn}_3\text{Cu}_{1-x}\text{Sn}_x\text{N}$  ( $x=0, 0.5$ ). The crystal structure of the compounds for  $x=0$  is tetragonal while  $x=0.5$  are cubic. That the cubic structure is recovered by Sn doping in  $\text{Mn}_3\text{Cu}_{1-x}\text{Sn}_x\text{N}$  may be the structural instability between the cubic and tetragonal phases the same as in  $\text{Mn}_3\text{Cu}_{1-x}\text{Ge}_x\text{N}$  [17]. This kind of local crystal structure distortion is an important factor for magnetic transition and broadening of MVE. For  $x=0$  the unit cell volume is  $58.799$  (Å $^3$ ) which is consistent with experiment

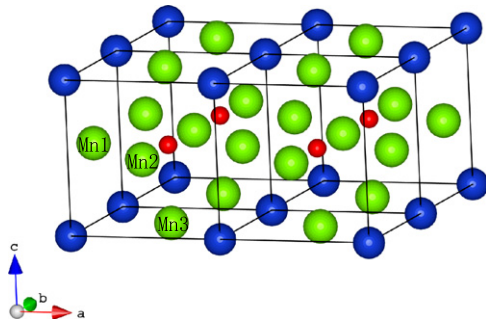


**Fig. 1.**  $\text{Mn}_3\text{CuN}$   $2 \times 2 \times 1$  supercell consists of 20 atoms with three inequivalent Mn sites designated as Mn1, Mn2 and Mn3, respectively. The green, blue, red spheres denote the Mn, Cu and N atoms, respectively. (For interpretation of the references to color in this figure legend, the reader is referred to the web version of this article.)

**Table 1**

Calculated structural parameters and total magnetic moments for  $\text{Mn}_3\text{Cu}_{1-x}\text{Sn}_x\text{N}$  ( $x=0, 0.5$ ) (in the parenthesis is experiment value).

Composition $x$	0	0.5
$a$ (Å)	3.908(3.912)	3.923
$b$ (Å)	3.908(3.912)	3.923
$c$ (Å)	3.850(3.852)	3.923
$V$ (Å $^3$ )	58.799(58.950)	60.375
$d_{\langle\text{N-Mn}\rangle}$ (Å)	1.944	1.961
$d_{\langle\text{Mn-Mn}\rangle}$ (Å)	2.749	2.774
$d_{\langle\text{Cu-Mn}\rangle}$ (Å)	2.749	2.774
$d_{\langle\text{Sn-Mn}\rangle}$ (Å)	–	2.774
$\mu_T$ ( $\mu_B$ /f.u.)	0.41	0.03

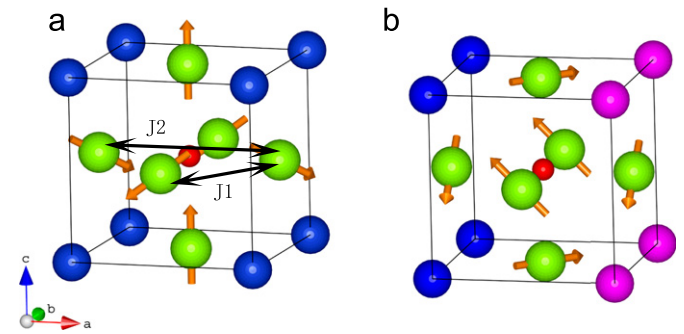


**Fig. 2.** (a) Calculated magnetic structure of  $\text{Mn}_3\text{CuN}$ . (b)  $\Gamma^{5g}$ -type antiferromagnetic structure of  $\text{Mn}_3\text{Cu}_{0.5}\text{Sn}_{0.5}\text{N}$ . The green, blue, red and purple red spheres denote the Mn, Cu, N and Sn atoms, respectively. (For interpretation of the references to color in this figure legend, the reader is referred to the web version of this article.)

$58.950$  (Å $^3$ ) [22]. The unit cell volume increases with  $x=0.5$ . The increase of the cell volume can be explained by the ionic radius of Sn being larger than that of Cu in the compounds. The average nearest-neighbor bond distance of  $d_{\langle\text{N-Mn}\rangle}$ ,  $d_{\langle\text{Mn-Mn}\rangle}$ ,  $d_{\langle\text{Cu-Mn}\rangle}$  and  $d_{\langle\text{Sn-Mn}\rangle}$  also increase with the  $x$  increasing. The value of total magnetic moment ( $\mu_T$ ) for  $\text{Mn}_3\text{CuN}$  is  $0.41 \mu_B$  and the total magnetic direction is along the *c* axis which is FM state. For  $\text{Mn}_3\text{Cu}_{1-x}\text{Sn}_x\text{N}$ , the total magnetic is small and negligible. Those results are consistent with experiments.

Fig. 2 shows the calculated magnetic structure of  $\text{Mn}_3\text{CuN}$  and  $\Gamma^{5g}$ -type antiferromagnetic structure of  $\text{Mn}_3\text{Cu}_{0.5}\text{Sn}_{0.5}\text{N}$ . The ordering patterns imply that nearest-neighbor J1 and next-nearest-neighbor J2 are antiferromagnetic and ferromagnetic, respectively. This can be explained that the nitrogen atom in the  $\text{Mn}_3\text{CuN}$  structure, with 2p orbit, can hybrid with the near-neighbour Mn  $e_g$ . Complementarily, near-neighbour Mn–Mn interactions are provided by orthogonal  $t_{2g}$  along the edges of the Mn octahedra. Thus both direct Mn–Mn and indirect Mn–N–Mn interactions are present. According to Goodenough–Anderson–Kanamori rules [23], in  $180^\circ$  Mn–N–Mn interactions, Mn cations with under half-filled d shell, are FM, whereas Mn–Mn interactions are AFM. So that J1 and J2 are antiferromagnetic and ferromagnetic coupled.

From Table 1, we can see that length of *c* is shorter than *a*, *b* in  $\text{Mn}_3\text{CuN}$ . That means  $180^\circ$  Mn–N–Mn FM parallelling *c* is stronger than *a*, *b*. Thus the total magnetic moments is along *c*. At the same time, we notice that corner-shared octahedra of Mn with AFM nearest-neighbor interactions are known to have three-dimensionally frustrated magnetic interactions. The effect of the spin geometrical frustration will indeed lead the non-collinear spin structures in  $\text{Mn}_3\text{CuN}$ .

Download English Version:

<https://daneshyari.com/en/article/1811253>

Download Persian Version:

<https://daneshyari.com/article/1811253>

[Daneshyari.com](https://daneshyari.com)